1521-0103/352/1/166–174$25.00
THE JOURNAL OF PHARMACOLOGY AND EXPERIMENTAL THERAPEUTICS

http://dx.doi.org/10.1124/jpet.114.219261
J Pharmacol Exp Ther 352:166–174, January 2015

Ophiopogonin D Attenuates Doxorubicin-Induced Autophagic Cell Death by Relieving Mitochondrial Damage In Vitro and In Vivo

Ying-Yu Zhang, Chen Meng, Xin-Mu Zhang, Cai-Hua Yuan, Ming-Da Wen, Zhong Chen, Da-Chuan Dong, Yan-Hong Gao, Chang Liu, and Zhao Zhang

Jiangsu Key Laboratory for Molecular and Medical Biotechnology, College of Life Science, Nanjing Normal University, Nanjing, China (Y.-Y.Z., C.M., C.-H.Y., M.-D.W., Z.C., D.-C.D., Y.-H.G., C.L., Z.Z.); Department of Clinical Medicine, Changchun Medical College, Changchun, China (Y.-Y.Z.); and Department of Biopharmaceutical, School of Pharmacy, Jilin University, Changchun, China (X.-M.Z)

Received August 11, 2014; accepted November 4, 2014

ABSTRACT

It has been reported that ophiopogonin D (OP-D), a steroidal glycoside and an active component extracted from *Ophiopogon japonicas*, promotes antioxidative protection of the cardiovascular system. However, it is unknown whether OP-D exerts protective effects against doxorubicin (DOX)-induced autophagic cardiomyocyte injury. Here, we demonstrate that DOX induced excessive autophagy through the generation of reactive oxygen species (ROS) in H9c2 cells and in mouse hearts, which was indicated by a significant increase in the number of autophagic vacuoles, LC3-II/LC3-I ratio, and upregulation of the expression of GFP-LC3. Pretreatment with OP-D partially attenuated the above phenomena, similar to the effects of treatment with 3-methyladenine. In addition, OP-D treatment significantly relieved the disruption of the mitochondrial membrane potential by antioxidative effects through downregulating the expression of both phosphorylated c-Jun N-terminal kinase and extracellular signal-regulated kinase. The ability of OP-D to reduce the generation of ROS due to mitochondrial damage and, consequently, to inhibit autophagic activity partially accounts for its protective effects in the hearts against DOX-induced toxicity.

Introduction

Doxorubicin (DOX), a potent anthracycline broad-spectrum antibiotic, is a widely used and successful anticancer drug for the treatment of hematologic malignancies and solid tumors (Minotti et al., 2004). Unfortunately, its long-term use is largely limited by its cumulative and dose-dependent cardiotoxicity, which may lead to chronic cardiomyopathy and eventually to life-threatening heart failure (Silber and Barber, 1995; Scott et al., 2011). Although intensive investigations into DOX-induced cardiotoxicity have been ongoing for decades, the precise mechanism underlying DOX-induced cardiotoxicity has not been completely clarified. Multiple possible mechanisms have been proposed, such as the formation of reactive oxygen species (ROS) in cardiomyocytes, direct DNA damage, loss of calcium homeostasis, apoptosis, and so on (Takemura and Fujiwara, 2007; Zhang et al., 2009). Among these, the overinduction of ROS production in cardiomyocyte mitochondria contributes mainly to the cardiac dysfunction and injury observed after DOX application (Tokarska-Schlattner et al., 2006; Stěrba et al., 2013). It is evident that there are several pathways for ROS generation upon DOX application. The redox cycling of DOX by NADH dehydrogenase generates a relatively small amount of ROS during drug metabolism, which in turn, or combined with DOX, directly leads to the induction of mitochondrial DNA lesions and, subsequently, respiratory chain failure as well as additional ROS liberation (Lebrecht and Walker, 2007; Wallace, 2007). In addition, the binding of DOX to the reductase domain of endothelial nitric oxide synthase is capable of converting the drug to an unstable semiquinone intermediate that favors ROS generation (Vasquez-Vivar et al., 1997; Neilan et al., 2007). There is no doubt that overproduced ROS initiated by DOX, as an

Y.-Y.Z. and C.M. contributed equally to this work.

This work was supported by the National Natural Science Foundation of China [Grants 30871228, 31171302]; the Opening Project of Jiangsu Province Key Laboratory for Molecular and Medical Biotechnology at Nanjing Normal University [Grant 2011MMBKF04]; and the project funded by the Priority Academic Program Development of Jiangsu Higher Education Institutions [Grant 164320H106]. Z.Z. and C.L. are the associate fellows at the Collaborative Innovation Center for Cardiovascular Disease Translational Medicine of Nanjing Medical University.
dx.doi.org/10.1124/jpet.114.219261.

ABBREVIATIONS: DCF-DA, 2′,7′-dichlorodihydrofluorescein diacetate; DMEM, Dulbecco's modified Eagle's medium; DOX, doxorubicin; EF, ejection fraction; ERK, extracellular signal-regulated kinase; FBS, fetal bovine serum; GAPDH, glyceraldehyde-3-phosphate dehydrogenase; JNK, c-Jun N-terminal kinase; LVFS, left ventricular fractional shortening; LVIDd, diastolic internal dimension of the left ventricle; LVIDs, systolic internal dimension of the left ventricle; 3-MA, 3-methyladenine; MAPK, mitogen-activated protein kinase; MTT, 3-[4,5-dimethylthiazol-2-yl]-2,5 diphenyl tetrazolium bromide; NAC, *N*-acetylcysteine; OP-D, ophiopogonin D; PBS, phosphate-buffered saline; ROS, reactive oxygen species; TEM, transmission electron microscopy.

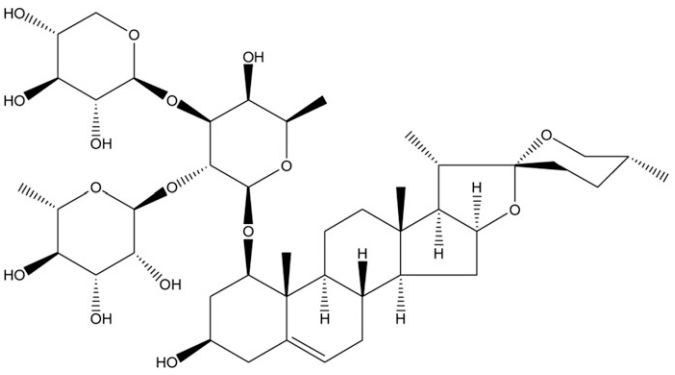

Fig. 1. Chemical structure of OP-D.

upstream inducer, triggers the activation of different signaling pathways, resulting in cardiomyocyte death through apoptosis, necrosis, and other forms. Autophagy is a dynamic process under physiologic conditions and is substantially enhanced in pathologic conditions, including heart hypertrophy, heart failure, or various types of stress. It is accepted that autophagy acts as a double-edged sword under specific circumstances, either protecting cells against death by removing protein aggregates and damaged organelles or mediating cell death via intense enhancement of autophagy (Nishida et al., 2009). Therefore, DOX is highly likely to lead to autophagic cardiomyocyte death because of ROS-induced mitochondrial impairment (Lu et al., 2009). In addition, taking mitochondria as the key subcellular organelle for DOX-associated cardiotoxicity into consideration, it could also be a crucial target during the use of cardioprotective agents together with DOX. At any rate, DOX remains one of the most effective drugs for the treatment of a wide variety of solid tumors and hematologic malignancies despite its dose-dependent cardiotoxic effects. Because the mechanisms underlying DOX-induced cardiotoxicity are complicated and not completely understood thus far, continued efforts need to be made in the further investigation of the molecular cardiopathogenesis resulting from DOX administration as well as the search for alternative cardioprotective therapies.

Ophiopogon japonicus is a well known traditional Chinese herbal medicine that has been used to treat cardiovascular diseases for thousands of years. Extensive studies have revealed that *O. japonicus* has potential beneficial effects on the cardiovascular system through various mechanisms, including antiarrhythmia, antioxidation, inhibiting platelet aggregation, improving microcirculation, and so on (Chen et al., 1990, 2013; Ichikawa et al., 2003; Kou et al., 2006). Ophiopogonin D (OP-D; Fig. 1), a steroidal glycoside and an active component extracted from *O. japonicus,* has been reported to be capable of protecting endothelial cells from H_2O_2-induced oxidative stress (Qian et al., 2010). However, it is largely unknown whether OP-D is able to protect cardiomyocytes from DOX-induced toxicity via its antioxidative effects. The purpose of this study was to investigate the effects of OP-D on DOX-induced cardiotoxicity and the possible mechanisms involved with a special focus on autophagy. Here, we report that DOX induced excessive autophagy through generation of ROS in H9c2 cells and in mouse hearts. However, OP-D treatment partially inhibited DOX-induced autophagic damage in cultured myocytes in vitro and in mouse hearts in vivo. In addition, OP-D treatment relieved the disruption of mitochondrial membrane potential by antioxidant effects through downregulating the expression of both phosphorylated c-Jun N-terminal kinase (JNK) and extracellular signal-regulated kinase (ERK). The ability of OP-D to reduce the generation of ROS due to mitochondrial damage and, consequently, to inhibit autophagic activity partially account for its heart protective effects against DOX-induced toxicity.

Materials and Methods

Reagents. DOX and 3-methyladenine (3-MA) were purchased from Sigma-Aldrich (St. Louis, MO). DOX was dissolved in Dulbecco's modified Eagle's medium (DMEM) at a concentration of 100 μM and stored as aliquots at −20°C. 3-MA was used at a concentration of 2.5 mM. OP-D was purchased from Tsumura (Tokyo, Japan) and dissolved in dimethylsulfoxide at a concentration of 10 mM. The stock solution was further diluted with culture medium to the final desired concentration. *N*-Acetylcysteine (NAC) was obtained from Sigma-Aldrich. Rabbit polyclonal anti-LC3 and SQSTM1 (p62) were supplied by Abcam (Cambridge, MA). The antibodies for JNK, p-JNK, ERK1/2, and p-ERK1/2 were purchased from Santa Cruz Biotechnology (Santa Cruz, CA). Monoclonal mouse anti–glyceraldehyde-3-phosphate dehydrogenase (GADPH) was purchased from Kang Chen Biotech (Shanghai, China). The mitochondrial membrane potential assay kit (JC-1) was purchased from Beyotime Biotechnology (Nantong, China).

Animals and Experimental Protocols. C57BL/6J mice were kept under standard laboratory conditions. The animal protocols used in this study were approved by the Animal Center of Nanjing Normal University and conform to the regulations for the administration of affairs concerning experimental animals issued by the Institutional

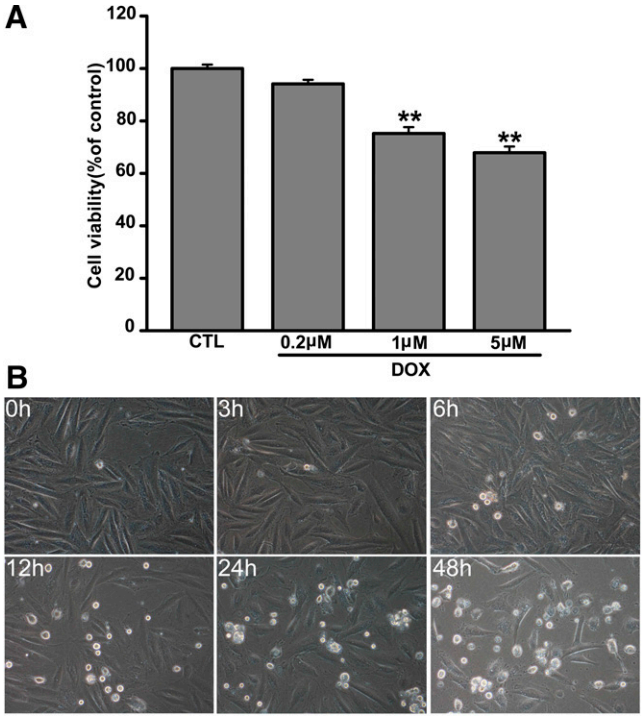

Fig. 2. Cytotoxic effects of DOX on H9c2 cells as measured by the MTT assay. (A) Measurement of cell viability after treatment with 0.2, 1, and 5 μM DOX for 24 hours. (B) Representative phase-contrast photomicrographs of H9c2 cells under the condition of 1 μM DOX exposure for the indicated time. $^{**}P < 0.01$ versus control (CTL).

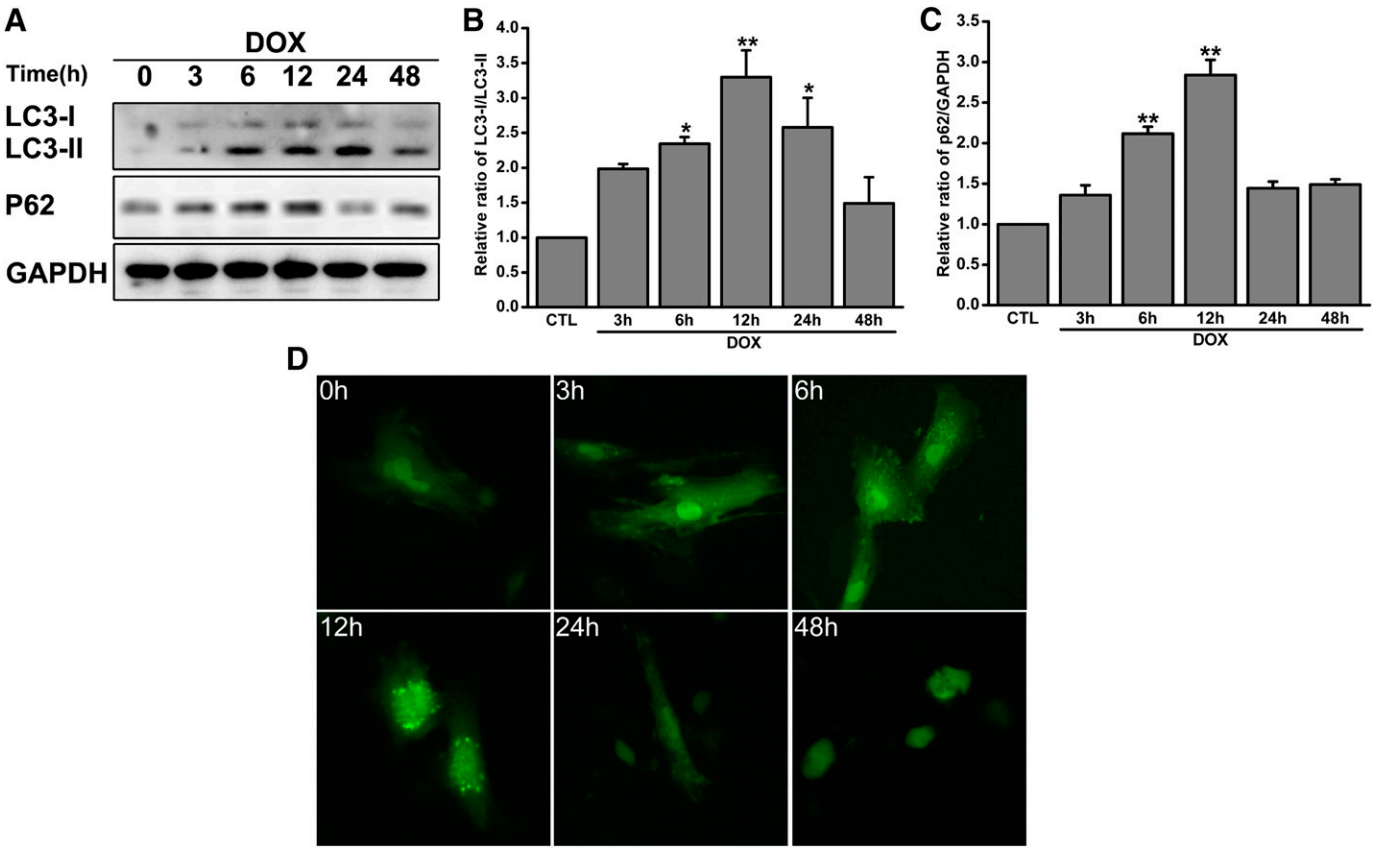

Fig. 3. DOX induces autophagy in H9c2 cells. (A) Representative Western blot depicting the levels of LC3-I, LC3-II, and p62 in 1 μM DOX-treated H9c2 cells at different time periods. (B and C) Graphs presenting summarized data from three independent experiments. Relative protein abundance was normalized to GAPDH. (D) GFP-LC3 punctate structures or dots were evident in H9c2 cells treated with 1 μM DOX for different time periods using fluorescence microscopy. $^{*}P < 0.05$; $^{**}P < 0.01$ versus CTL.

Animal Care and Use Committee from Jiangsu Province and the Ministry of Science and Technology in the People's Republic of China.

Male 8-week-old mice, weighing 20~25 g, were randomly assigned to four groups with 7 mice in each: 1) saline, 2) DOX (2 mg/kg), 3) OP-D (10 mg/kg), and 4) DOX plus OP-D. All of the mice in each group were subjected to an intraperitoneal injection every other day for a total of 7 days. In the 4th group, administration of OP-D was performed 1 day before DOX injection. At the end of the experiment period, the mice were killed by injection of a lethal dose of sodium phenobarbital, and their hearts were rapidly removed for protein extraction or transmission electron microscopy.

Cell Culture. H9c2 rat heart-derived embryonic myocytes were purchased from the Cell Bank of the Chinese Academy of Science (Beijing, China). Cells were grown in DMEM supplemented with 10% inactivated fetal bovine serum (FBS), 500 μg/ml penicillin, and 500 μg/ml streptomycin at 37°C in a humidified incubator with 5% CO_2.

Cell Viability Assay. Cells were seeded into 96-well plates at a density of 3×10^4 cell per well and were subjected to the modified MTT (3-[4,5-dimethylthiazol-2-yl]-2,5 diphenyl tetrazolium bromide) assay. Briefly, cells were allowed to adhere in 96-well plates overnight in 10% FBS containing medium before being subjected to the indicated drug treatment concentration. OP-D was added to H9c2 cells at the final concentration 12 hours before treatment with DOX. Then, the medium was replaced with fresh medium containing 1 μM DOX for the indicated time for each experiment. At appropriate time intervals, 50 μl of MTT solution was added to each well and incubated in 37°C for 4 hours. The medium was then carefully removed, and formazan crystals were dissolved by adding 150 μl of dimethylsulfoxide for each well. The optical density was measured at 570 nm in a microplate reader (Thermo Scientific, Waltham, MA).

Transfection. Cells were plated in 6-well plates (1.0×10^6) and refreshed with serum- and antibiotic-free DMEM 12 hours before transfection. Transient transfection of GFP-LC3 plasmid (1 μg/well) was performed using Lipofectamine 2000 (Invitrogen, Grand Island, NY) according to the manufacturer's instructions. Transfected cells were cultured for 12 hours, and the medium was then replaced with fresh medium supplemented with 10% FBS. Another 36 hours later, the cells were treated with DOX in the absence or presence of 3-MA or OP-D for the indicated time.

Western Blot Assay. H9c2 cells were lysed in radioimmunoprecipitation assay buffer containing 50 mM Tris/HCl (pH 8.0), 150 mM NaCl, 1% Nonidet-P40, 1% sodium deoxycholate, 0.1% SDS, 0.1 mM dithiothreitol, 0.05 mM phenylmethylsulfonyl fluoride, and a protease inhibitor cocktail. An equal quantity of protein was subjected to SDS-PAGE on 8~15% polyacrylamide gel and transferred to a polyvinylidene difluoride membrane. The membrane was blocked for 1 hour with blocking buffer containing 5% fat-free dry milk Tris-buffered saline/Tween 20 (0.1% Tween 20 in Tris-buffered saline), followed by incubation with the appropriate primary antibodies in blocking buffer overnight at 4°C. Then, the membrane was washed three times with Tris-buffered saline/Tween 20 for 30 minutes and incubated with horseradish peroxidase–conjugated secondary antibody (Bioworld Technology, St. Louis, MN) at room temperature for 1 hour. The immunoreactive signals were visualized with a FluorChem E System (Cell Biosciences, San Jose, CA).

Mitochondrial Membrane Potential Assay. The mitochondrial membrane potential was measured using a mitochondrial membrane potential assay kit (Beyotime Biotechnology, Jiangsu, China). Briefly, H9c2 cells were seeded in a 6-well plate and treated with the indicated concentration of OP-D for 12 hours. The medium was replaced with

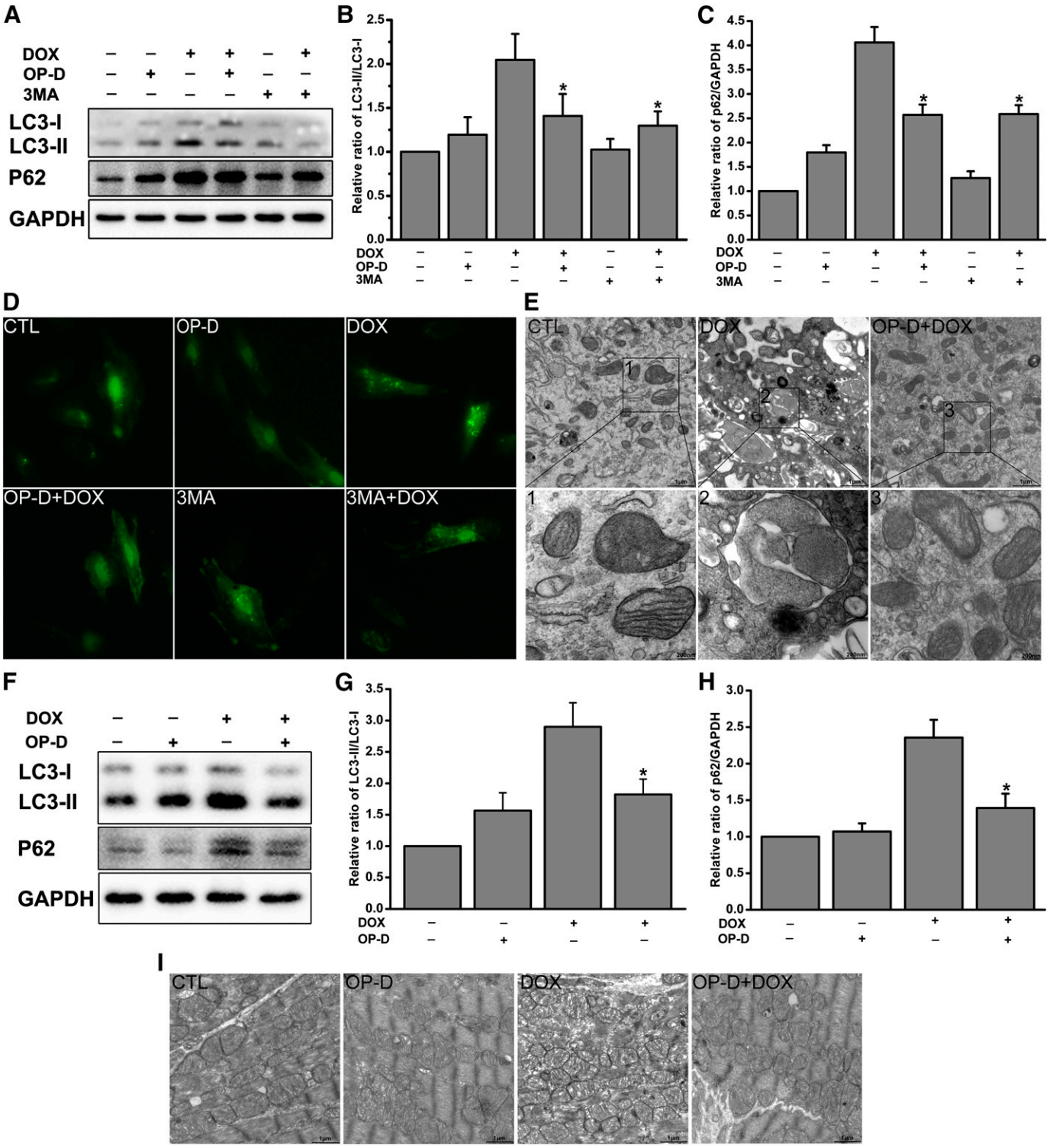

Fig. 4. OP-D protects myocardiocytes against DOX-induced autophagy in vitro and in vivo. (A) Representative Western blot showing expression levels of LC3-I, LC3-II, and p62 in H9c2 cells exposed to DOX for 12 hours in the presence or absence of 1 μM OP-D or 2.5 mM 3-MA. (B and C) A summary of gray densitometric analysis results from the experiments as illustrated in (A). Relative protein abundance was normalized to GAPDH. (D) Fluorescence microscopy images displaying GFP-LC3 direct fluorescence from 1 μM DOX-treated H9c2 cells without or with pretreatment with 1 μM OP-D or 2.5 mM 3-MA for 12 hours. (E) Representative images obtained by TEM illustrating ultrastructural changes in H9c2 cells under the condition of control, DOX alone, and DOX plus OP-D. (F) Representative Western blot demonstrating the expression levels of LC3-I, LC3-II, and p62 in mouse heart tissues obtained from the mice who received vehicle, DOX only, and DOX plus OP-D injection. (G and H) Depict a summary of densitometric analysis from the experiments as revealed in (F). The relative protein abundance was normalized to GAPDH. (I) Representative images showing mitochondrial injuries in mouse myocardia under the same conditions as in (F). *$P < 0.05$ DOX plus OP-D versus DOX alone.

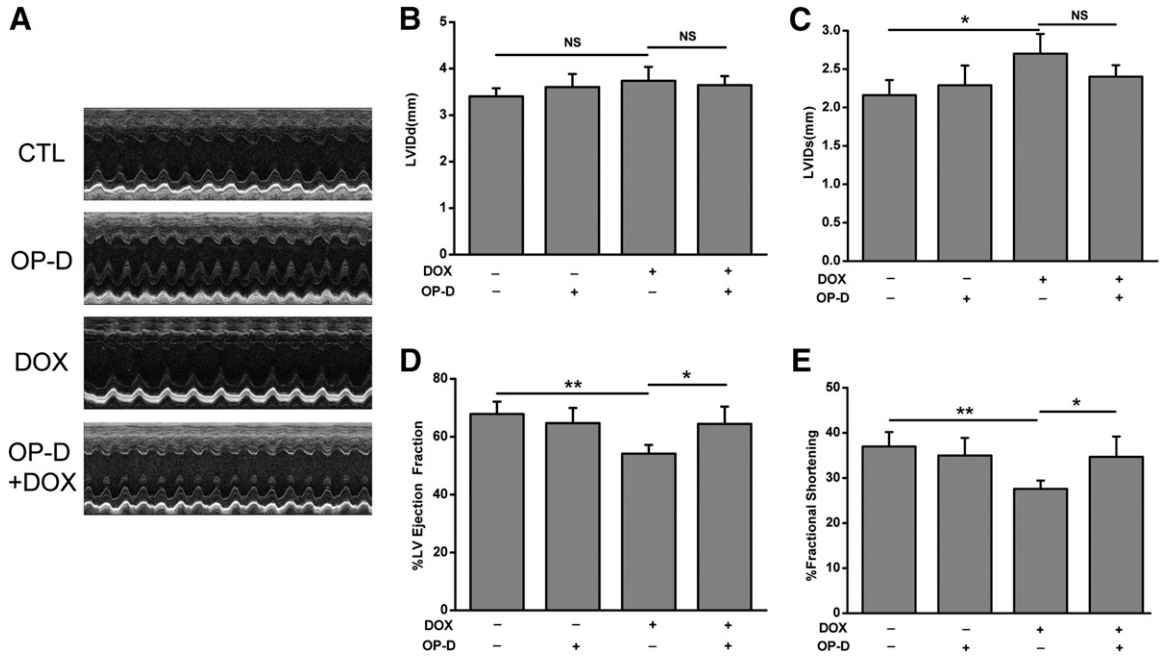

Fig. 5. Effects of OP-D on DOX-induced abnormal cardiac function. (A) Representative echocardiogram recorded from the mice in control and different treatment groups. (B–E) Summarized data for cardiac functional assay as measured by LVIDd, LVIDs, and EF%, as well as LVFS%. NS, not significant. $^{*}P < 0.05$; $^{**}P < 0.01$.

fresh medium containing DOX for the indicated time. The cells were harvested, loaded with 1 μM JC-1 in the dark at 37°C for 20 minutes according to the manufacturer's protocol, and washed twice with phosphate-buffered saline (PBS). The cells labeled with JC-1 were determined by flow cytometry using a Guava EasyCyte system (Guava Technologies, Hayward, CA).

Determination of Intracellular ROS. For analysis of ROS, the DCF-DA probe was used. Briefly, cells treated as described above were incubated with 10 μM DCF-DA (2′,7′-dichlorodihydrofluorescein diacetate) at 37°C for 30 minutes. After incubation with the fluorochrome, cells were washed and resuspended in cold PBS. The fluorescence intensity of 2,7-dichlorofluorescin formed by the reaction of DCF-DA with intracellular ROS of more than 5000 viable cells was analyzed by flow cytometry using a Guava EasyCyte system (Guava Technologies).

Electron Microscopy. H9c2 cells were collected by centrifugation and three washes with PBS. Then, they were fixed with 4% glutaraldehyde. Next, the cells were post-fixed with 1% perosmic acid and dehydrated with acetone. Ultrathin sections were placed on 400 mesh grids and double stained with uranyl acetate and lead citrate. The sections were observed under transmission electron microscopy (TEM; JEM1230; Jeol, Tokyo, Japan).

Statistical Analysis. All of the data are presented as the mean ± S.E.M. One-way analysis of variance with Tukey's post tests was used to determine the significance of differences between the control and test groups. Originpro 8.0 software was used for statistical analysis. A value of $P < 0.05$ was considered to indicate a statistically significant difference.

Results

DOX Induces Cytotoxicity in H9c2 Cells. To determine the cytotoxic effect of DOX on H9c2 cells, an MTT assay was performed. As shown in Fig. 2A, the viability of H9c2 cells was obviously decreased upon DOX exposure for 48 hours at concentrations of 0.2, 1, and 5 μm. In addition, when 1 μm DOX was applied, the number of dead cells was significantly increased with the time of drug exposure (Fig. 2B), suggesting both concentration- and time-dependent cytotoxicity.

DOX Induces Autophagy in H9c2 Cells. H9c2 cells were subjected to treatment with DOX for different time periods, and then the expression of LC3-I and LC3-II was examined by immunoblotting. The results indicated that the ratio of LC3-II/LC3-I was increased with the time of DOX exposure and reached a peak at 12 to 24 hours (Fig. 3, A and B). The expression profile of p62 paralleled that of the ratio for LC3-II/LC3-I (Fig. 3C). To further confirm the role of DOX in autophagy induction, autophagosome formation in H9c2 cells was evaluated using GFP-LC3 puncta. A diffuse staining pattern of GFP-LC3 was observed in control cardiomyocytes, whereas GFP-LC3 punctate structures were observed in the cells treated with DOX (Fig. 3D). Accordingly, DOX-induced ultrastructural changes in H9c2 cells characterized as more vacuolar components containing mitochondria or other cellular organelles inside were observed by TEM examination (see the next section).

OP-D Attenuates DOX-Induced Autophagy In Vitro and In Vivo. To examine the effects of OP-D on the DOX-induced autophagy, both DOX-treated H9c2 cells and mouse heart tissues were collected for Western blots or morphologic analysis. As shown in Fig. 4A, DOX-induced increases in the ratio of LC3-II/LC3-I and p62 expression were significantly attenuated when the cells were pretreated with 1 μm OP-D or the autophagy inhibitor 3-MA (2.5 mM; Fig. 4, B and C), suggesting that OP-D pretreatment helps cardiac cells stave off the autophagosomal formation induced by DOX. Consistently, the relieving effects of OP-D on DOX-induced induction of autophagy in H9c2 cells were further confirmed by either quantification of GFP-LC3 puncta (Fig. 4D) or autophagic vacuoles (Fig. 4E) using fluorescence or TEM examination. There were fewer autophagosomes in the cells pretreated with OP-D for 12 hours compared with those treated with DOX

alone. Of note, the relieving effects of OP-D on DOX-induced autophagy were addressed in the hearts obtained from the mice that received DOX injections. Western blot analysis indicated that the increases in the ratio of LC3-II/LC3-I and p62 expression in response to DOX administration were significantly attenuated after pretreatment with OP-D (10 mg/kg before DOX administration; Fig. 4, F–H). Consequently, obvious cardiac injury in mice subjected to DOX injection was documented in the TEM examination, with swollen mitochondria and the rupture of mitochondrial cristae in particular. In contrast, an improved myocardial morphology was observed in mice receiving OP-D before DOX injection (Fig. 4I).

OP-D Protects against DOX-Induced Cardiac Dysfunction. To evaluate the protective effects of OP-D on cardiac function in mice, echocardiography was performed at the final dose of DOX and OP-D injections. The representative echocardiograms of the four groups are shown in Fig. 5A. The quantitative percentages of the diastolic internal dimension of the left ventricle (LVIDd), the systolic internal dimension of the left ventricle (LVIDs), ejection fraction of the left ventricle (EF%) and left ventricular fractional shortening (LVFS%), obtained for all of the four groups, are summarized in Fig. 5B. In control and OP-D alone group, the LVIDd, LVIDs, EF%, and LVFS% were unchanged. In contrast, slight increases in both LVIDd and LVIDs and obvious decreases in both EF and LVFS were detected in DOX-treated mice, which reflect significant cardiac contractile dysfunction. However, the reductions in EF and LVFS observed in DOX-treated mice were reversed in the OP-D plus DOX-treated group, indicating that OP-D protects against DOX-induced cardiac dysfunction.

OP-D Attenuates DOX-Induced ROS Accumulation in H9c2 Cells. To evaluate the protective effects of OP-D on DOX-induced mitochondrial damage, ROS accumulation, and the resultant autophagic cell death, we next measured the mitochondrial membrane potential and the ROS content using a flow cytometer. The results are shown in Fig. 6. A significant disruption of mitochondrial membrane potential in H9c2 cells was observed upon exposure to DOX, as determined with the JC-1 fluorescent probes, whereas the disruption of mitochondrial membrane potential was significantly prevented either in the presence of 1 μm OP-D or in the presence of

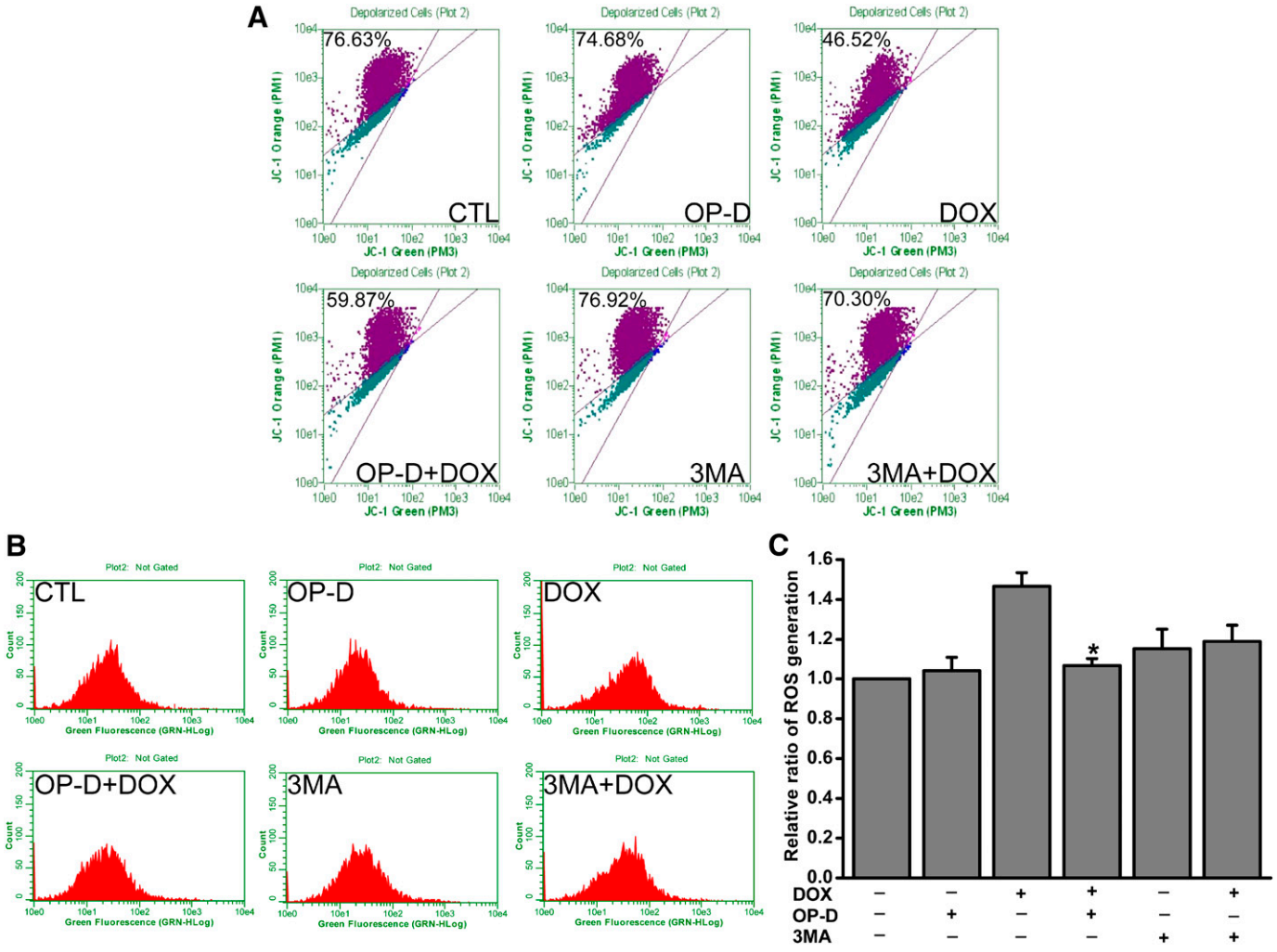

Fig. 6. OP-D protects H9c2 cells against DOX-induced oxidative stress. (A) Flow cytometric patterns of H9c2 cells stained with JC-1. H9c2 cells were exposed to 1 μM OP-D or 2.5 mM 3-MA for 12 hours before 1 μM DOX administration and then stained with JC-1 to measure mitochondrial membrane potential ($\Delta\Psi$m) via flow cytometry. (B) Assay of ROS accumulation in H9c2 cells under the different conditions. The cells were subjected to the same treatment as in (A) and then incubated with DCF-DA to determine the ROS content via flow cytometry. (C) A summary of gray densitometric analysis from 3 independent experiments. $^*P < 0.05$ versus DOX group.

2.5 mM 3-MA (Fig. 6A). Moreover, the increased ROS production observed in DOX-treated H9c2 cells was completely blocked by pretreatment of OP-D or 3-MA as measured with a specific fluorescent dye, DCF-DA, strongly suggesting that the OP-D produced a cytoprotective effect against DOX-induced autophagic damage through its antioxidative action (Fig. 6B).

OP-D Inhibits the Activation of JNK and ERK in H9c2 Cells in Response to DOX Administration. To clarify whether mitogen-activated protein kinase (MAPK) signaling pathways play any role in DOX-induced autophagy in H9c2 cells, we finally tracked the phosphorylation of JNK (p-JNK), ERK1/2 (p-ERK), and P38 (p-P38) by Western blotting control cells and the cells pretreated with 1 μm OP-D or 1 mM NAC for 12 hours, followed by treatment with 1 μm DOX for another 12 hours. Dramatically enhanced expression of p-JNK, p-ERK1/2, and p-P38 but not total JNK, ERK, and P38 were detected in DOX-treated group by Western blot analysis, implying a role for all MAPK family members in mediating DOX-induced induction of autophagy in cardiomyocytes. However, the DOX-induced activation of JNK and ERK was partially inhibited by pretreatment with either OP-D or NAC, with the exception of P38 (Fig. 7, A and C). Collectively, these results strongly demonstrated that OP-D has protective effects against DOX-induced mitochondrial damage and the induction of autophagy in cardiomyocytes in addition to demonstrating that the inhibition of JNK and ERK1/2 but not P38 was, at least in part, involved in the protective mechanism.

Discussion

DOX and other anthracyclines continue to play an undisputed role in the treatment of many forms of cancer, but the issue of their cardiotoxicity has not been solved thus far (Cortes-Funes and Coronado, 2007). In this regard, exploring proper prevention and treatment strategies is urgently required. Based on the fact that mitochondrial dysfunction, resultant free radical generation, and oxidative stress are the main triggers in DOX-induced cardiotoxicity, protective strategies have focused on administering drugs or natural compounds that improve the antioxidant defenses of cardiomyocytes against DOX-derived oxidative stress. We described here for the first time that OP-D is capable of protecting cardiomyocytes against DOX-induced autophagic injury through its antioxidative effect. The inhibition of the JNK and ERK pathways associated with OP-D application may account for this protective process.

A line of evidence indicates that the increase in ROS production stimulates autophagy in cardiomyocytes, serving

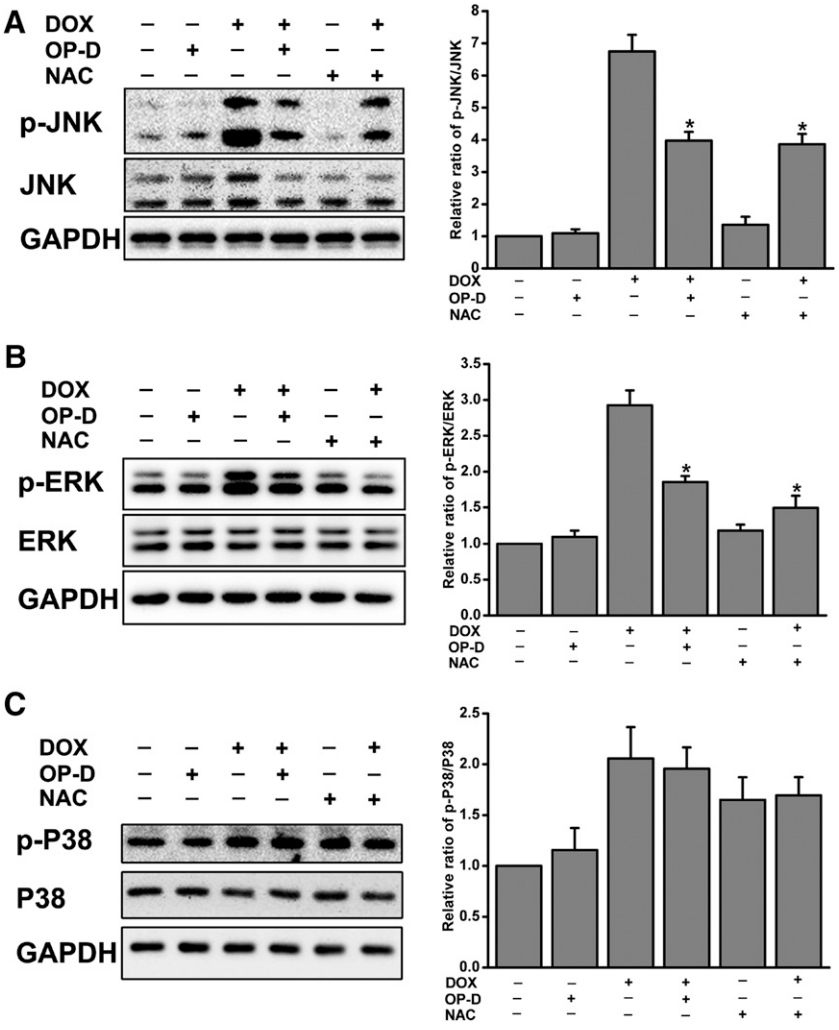

Fig. 7. Effects of OP-D on DOX-induced MAPKs activation in H9c2 cells. (A) H9c2 cells were treated with 1 μM DOX for 12 hours in the absence or presence of a 12-hour pretreatment of 1 μM OP-D or 1 mM NAC. The phosphorylation of JNK was detected by Western blot analysis. (B and C) H9c2 cells were subjected the same treatment and detection as in (A) except using anti–phospho-ERK1/2 and anti–phospho-P38 antibodies for detection, respectively. The bar graphs in (A), (B), and (C) show the summary of gray densitometric analysis from the experiments as indicated in blots. *$P < 0.05$ versus DOX group.

as a quality-control mechanism to protect cells from oxidative injury by limiting further ROS production (Yuan et al., 2009). However, sustained induction of autophagy may lead to the opposite direction, causing cell death (Huang et al., 2011; Xu et al., 2012). It has been found that altered autophagy contributes to various heart diseases, including cardiac hypertrophy, heart failure (Nakai et al., 2007; Matsui et al., 2008), and DOX-induced cardiotoxicity (Kanamori et al., 2011; Li et al., 2014). However, it remains unclear whether autophagy plays a beneficial or detrimental role in the heart. In the present study, DOX-induced autophagy was documented both in cultured H9c2 cells and in mouse hearts, as indicated by the significant accumulation of LC3-II and p62 as well as the formation of autophagic ultrastructure. Of note, DOX-induced autophagy was paralleled with a significant decrease in cell viability, dysfunction of mitochondria, and increase in the ROS production, whereas these effects were blocked by pretreatment with the autophagy inhibitor 3-MA, strongly suggesting an occurrence of excessive activation of autophagy, which leads to cell death in cardiomyocytes upon DOX administration. Our observation that activation of autophagy mediates DOX-induced cardiotoxicity is not new. Similar results were previously reported in a DOX-induced rat model (Lu et al., 2009) and neonatal rat ventricular cardiomyocytes (Kobayashi et al., 2010; Chen et al., 2011). Thus, the present findings appear to provide additional evidence that links autophagic cell death to DOX-induced cardiotoxicity. It is noteworthy that the concentration of DOX used in our study was 1 μM, which is only one-fifth of that reported by Wang et al. (2012), suggesting that the lower concentration of DOX is capable of causing autophagic injury to cardiomyocytes. More important findings in the present study are the protective effects of OP-D against DOX-induced autophagic damage in either cultured H9c2 cells or mice receiving DOX injection. These effects, similar to 3-MA, were indicated by OP-D pretreatment-associated attenuation of autophagic cell death and a significant increase in cell viability.

It has been well documented that mitochondrial ROS is involved primarily in DOX-induced irreversible and cumulative cardiomyopathy (Davies and Doroshow, 1986). Considering the role of ROS signaling in the induction of autophagy in response to DOX treatment, we examined the intracellular ROS content and the change of mitochondrial membrane potential and found an increased ROS level and disrupted mitochondrial membrane potential, which implicates drug-induced mitochondrial damage and oxidative stress in cardiomyocytes. Cells have developed various protective mechanisms against oxidative stress, in which autophagy plays a dynamic role (Nishida et al., 2009; Yuan et al., 2009). Autophagy, which can be induced by ROS accumulation, has the capability to remove damaged proteins and organelles and thus maintains cellular homeostasis, whereas severe autophagy leads to cytotoxicity and autophagic cell death (Nishida et al., 2009; Huang et al., 2011). In this context, there is no doubt that our observation of DOX-induced autophagic damage, both in vitro and in vivo, was triggered by ROS accumulation. It is a remarkable fact that OP-D pretreatment reduced the level of ROS and the extent of disruption of the mitochondrial membrane potential in DOX-treated cardiac cells in vitro and in vivo, which strongly suggests that OP-D may achieve its protective effects for cardiac cells by scavenging ROS and relieving oxidative stress, which is in line with its role in H_2O_2-induced endothelial injury as reported by Qian et al. (2010). Therefore, it is necessary to further investigate the changes in the expression of antioxidant genes and activity of antioxidant enzymes, as well as the other pathways involved in OP-D protection.

Previous studies have demonstrated the role of MAPK signaling pathways in mediating DOX-induced cardiotoxicity via intracellular ROS production (Lou et al., 2005; Spallarossa et al., 2006). In response to DOX application, however, the findings concerning changes among this set of MAPK family members conflict based on the reports of different groups. For example, Liu et al. (2008) reported observing increased p-ERK1/2 but unchanged p-JNK and p-P38 in DOX-treated H9c2 cells. In another report, P38 MAPK was demonstrated to contribute to DOX-induced inflammation and cytotoxicity in H9c2 cardiac cells (Guo et al., 2013). These findings might be attributed to the regulation of MAPK being dependent on the time of DOX treatment and the different experimental conditions used. In this study, our results indicate that the level of p-JNK, p-ERK, and p-P38 obviously increased in a time-dependent manner with DOX treatment, implicating all of these kinases in DOX-induced cardiotoxicity, whereas DOX-induced activation of JNK and ERK1/2, but not P38, was obviously inhibited by OP-D pretreatment, which implies that both JNK and ERK are the major MAPKs involved in the antioxidant effects of OP-D. Furthermore, we should state the fact that OP-D pretreatment is incapable of completely reversing the DOX-induced impairment of cardiac viability. The possible explanations are that the mechanisms underlying DOX-induced cytotoxicity are complicated and involved in multiple signaling pathways.

Taken together, our results prove, for the first time, the protective effects of OP-D against DOX-induced autophagic cardiomyocyte injury in vitro and in vivo. Scavenging ROS and relieving oxidative stress by inhibiting DOX-induced activation of JNK and ERK1/2 contribute to this process, at least in part (Fig. 8). Therefore, OP-D appears to be an effective protective agent for patients who undergo DOX administration as an effective antineoplastic chemotherapy.

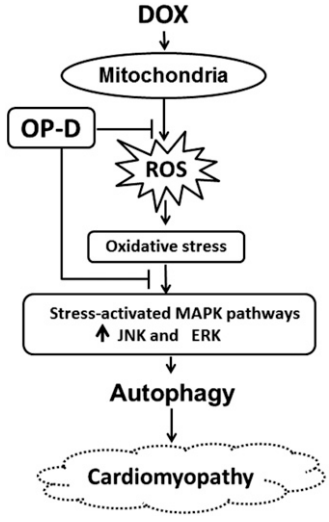

Fig. 8. Schematic description of DOX-induced autophagic cardiomyocyte injury and the protective effects of OP-D. DOX induces oxidative stress via production of ROS in mitochondria in cardiomyocytes, which causes the activation of JNK and ERK MAPKs linked with autophagy. OP-D attenuates DOX-induced autophagic cardiomyocyte injury via scavenging ROS and further inhibiting DOX-induced activation of JNK and ERK1/2.

Acknowledgments

The authors thank Dr. Li Liu for excellent technical assistance in the assessment of mouse cardiac function by echocardiography, and Dr. Yue-Hua Li and Kai-He Du for TEM examination.

Authorship Contributions

Participated in research design: Y.-Y. Zhang, Meng, Liu, Z. Zhang.

Conducted experiments: Y.-Y. Zhang, Meng, X.-M. Zhang,Yuan, Wen, Chen.

Contributed new reagents or analytic tools: Y.-Y. Zhang, Liu.

Performed data analysis: Meng, Dong, Gao.

Wrote or contributed to the writing of the manuscript: Y.-Y. Zhang, Meng, Liu, Z. Zhang.

References

Chen K, Xu X, Kobayashi S, Timm D, Jepperson T, and Liang Q (2011) Caloric restriction mimetic 2-deoxyglucose antagonizes doxorubicin-induced cardiomyocyte death by multiple mechanisms. *J Biol Chem* **286**:21993–22006.

Chen M, Yang ZW, Zhu JT, Xiao ZY, and Xiao R (1990) [Anti-arrhythmic effects and electrophysiological properties of Ophiopogon total saponins]. *Zhongguo Yao Li Xue Bao* **11**:161–165.

Chen X, Tang J, Xie W, Wang J, Jin J, Ren J, Jin L, and Lu J (2013) Protective effect of the polysaccharide from Ophiopogon japonicus on streptozotocin-induced diabetic rats. *Carbohydr Polym* **94**:378–385.

Cortés-Funes H and Coronado C (2007) Role of anthracyclines in the era of targeted therapy. *Cardiovasc Toxicol* **7**:56–60.

Davies KJ and Doroshow JH (1986) Redox cycling of anthracyclines by cardiac mitochondria. I. Anthracycline radical formation by NADH dehydrogenase. *J Biol Chem* **261**:3060–3067.

Guo RM, Xu WM, Lin JC, Mo LQ, Hua XX, Chen PX, Wu K, Zheng DD, and Feng JQ (2013) Activation of the p38 MAPK/NF-κB pathway contributes to doxorubicin-induced inflammation and cytotoxicity in H9c2 cardiac cells. *Mol Med Rep* **8**: 603–608.

Huang J, Lam GY, and Brumell JH (2011) Autophagy signaling through reactive oxygen species. *Antioxid Redox Signal* **14**:2215–2231.

Ichikawa H, Wang X, and Konishi T (2003) Role of component herbs in antioxidant activity of shengmai san—a traditional Chinese medicine formula preventing cerebral oxidative damage in rat. *Am J Chin Med* **31**:509–521.

Kanamori H, Takemura G, Goto K, Maruyama R, Tsujimoto A, Ogino A, Takeyama T, Kawaguchi T, Watanabe T, and Fujiwara T, et al. (2011) The role of autophagy emerging in postinfarction cardiac remodelling. *Cardiovasc Res* **91**:330–339.

Kobayashi S, Volden P, Timm D, Mao K, Xu X, and Liang Q (2010) Transcription factor GATA4 inhibits doxorubicin-induced autophagy and cardiomyocyte death. *J Biol Chem* **285**:793–804.

Kou J, Tian Y, Tang Y, Yan J, and Yu B (2006) Antithrombotic activities of aqueous extract from Radix Ophiopogon japonicus and its two constituents. *Biol Pharm Bull* **29**:1267–1270.

Lebrecht D and Walker UA (2007) Role of mtDNA lesions in anthracycline cardiotoxicity. *Cardiovasc Toxicol* **7**:108–113.

Li S, Wang W, Niu T, Wang H, Li B, Shao L, Lai Y, Li H, Janicki JS, and Wang XL, et al. (2014) Nrf2 deficiency exaggerates doxorubicin-induced cardiotoxicity and cardiac dysfunction. *Oxid Med Cell Longev* **2014**:748524.

Liu J, Mao W, Ding B, and Liang CS (2008) ERKs/p53 signal transduction pathway is involved in doxorubicin-induced apoptosis in H9c2 cells and cardiomyocytes. *Am J Physiol Heart Circ Physiol* **295**:H1956–H1965.

Lou H, Danelisen I, and Singal PK (2005) Involvement of mitogen-activated protein kinases in adriamycin-induced cardiomyopathy. *Am J Physiol Heart Circ Physiol* **288**:H1925–H1930.

Lu L, Wu W, Yan J, Li X, Yu H, and Yu X (2009) Adriamycin-induced autophagic cardiomyocyte death plays a pathogenic role in a rat model of heart failure. *Int J Cardiol* **134**:82–90.

Matsui Y, Kyoi S, Takagi H, Hsu CP, Hariharan N, Ago T, Vatner SF, and Sadoshima J (2008) Molecular mechanisms and physiological significance of autophagy during myocardial ischemia and reperfusion. *Autophagy* **4**:409–415.

Minotti G, Menna P, Salvatorelli E, Cairo G, and Gianni L (2004) Anthracyclines: molecular advances and pharmacologic developments in antitumor activity and cardiotoxicity. *Pharmacol Rev* **56**:185–229.

Nakai A, Yamaguchi O, Takeda T, Higuchi Y, Hikoso S, Taniike M, Omiya S, Mizote I, Matsumura Y, and Asahi M, et al. (2007) The role of autophagy in cardiomyocytes in the basal state and in response to hemodynamic stress. *Nat Med* **13**:619–624.

Neilan TG, Blake SL, Ichinose F, Raher MJ, Buys ES, Jassal DS, Furutani E, Perez-Sanz TM, Graveline A, and Janssens SP, et al. (2007) Disruption of nitric oxide synthase 3 protects against the cardiac injury, dysfunction, and mortality induced by doxorubicin. *Circulation* **116**:506–514.

Nishida K, Kyoi S, Yamaguchi O, Sadoshima J, and Otsu K (2009) The role of autophagy in the heart. *Cell Death Differ* **16**:31–38.

Qian J, Jiang F, Wang B, Yu Y, Zhang X, Yin Z, and Liu C (2010) Ophiopogonin D prevents H2O2-induced injury in primary human umbilical vein endothelial cells. *J Ethnopharmacol* **128**:438–445.

Scott JM, Khakoo A, Mackey JR, Haykowsky MJ, Douglas PS, and Jones LW (2011) Modulation of anthracycline-induced cardiotoxicity by aerobic exercise in breast cancer: current evidence and underlying mechanisms. *Circulation* **124**:642–650.

Silber JH and Barber G (1995) Doxorubicin-induced cardiotoxicity. *N Engl J Med* **333**:1359–1360.

Spallarossa P, Altieri P, Garibaldi S, Ghigliotti G, Barisione C, Manca V, Fabbi P, Ballestrero A, Brunelli C, and Barsotti A (2006) Matrix metalloproteinase-2 and -9 are induced differently by doxorubicin in H9c2 cells: The role of MAP kinases and NAD(P)H oxidase. *Cardiovasc Res* **69**:736–745.

Stěrba M, Popelová O, Vávrová A, Jirkovský E, Kovaříková P, Geršl V, and Simůnek T (2013) Oxidative stress, redox signaling, and metal chelation in anthracycline cardiotoxicity and pharmacological cardioprotection. *Antioxid Redox Signal* **18**:899–929.

Takemura G and Fujiwara H (2007) Doxorubicin-induced cardiomyopathy from the cardiotoxic mechanisms to management. *Prog Cardiovasc Dis* **49**:330–352.

Tokarska-Schlattner M, Zaugg M, Zuppinger C, Wallimann T, and Schlattner U (2006) New insights into doxorubicin-induced cardiotoxicity: the critical role of cellular energetics. *J Mol Cell Cardiol* **41**:389–405.

Vásquez-Vivar J, Martasek P, Hogg N, Masters BS, Pritchard KA, Jr, and Kalyanaraman B (1997) Endothelial nitric oxide synthase-dependent superoxide generation from adriamycin. *Biochemistry* **36**:11293–11297.

Wallace KB (2007) Adriamycin-induced interference with cardiac mitochondrial calcium homeostasis. *Cardiovasc Toxicol* **7**:101–107.

Wang XY, Yang CT, Zheng DD, Mo LQ, Lan AP, Yang ZL, Hu F, Chen PX, Liao XX, and Feng JQ (2012) Hydrogen sulfide protects H9c2 cells against doxorubicin-induced cardiotoxicity through inhibition of endoplasmic reticulum stress. *Mol Cell Biochem* **363**:419–426.

Xu X, Chen K, Kobayashi S, Timm D, and Liang Q (2012) Resveratrol attenuates doxorubicin-induced cardiomyocyte death via inhibition of p70 S6 kinase 1-mediated autophagy. *J Pharmacol Exp Ther* **341**:183–195.

Yuan H, Perry CN, Huang C, Iwai-Kanai E, Carreira RS, Glembotski CC, and Gottlieb RA (2009) LPS-induced autophagy is mediated by oxidative signaling in cardiomyocytes and is associated with cytoprotection. *Am J Physiol Heart Circ Physiol* **296**:H470–H479.

Zhang YW, Shi J, Li YJ, and Wei L (2009) Cardiomyocyte death in doxorubicin-induced cardiotoxicity. *Arch Immunol Ther Exp (Warsz)* **57**:435–445.

Address correspondence to: Zhao Zhang, Jiangsu Key Laboratory for Molecular and Medical Biotechnology, College of Life Science, Nanjing Normal University, 1 Wenyuan Road, Nanjing 210023, China. E-mail: zhangzhao@njnu.edu.cn or zhangzhaolab@163.com